Available online at www.CivileJournal.org

Civil Engineering Journal

(E-ISSN: 2476-3055; ISSN: 2676-6957)

Vol. 12, No. 04, April, 2026

Influence of Rock Bolt Support Parameters on Geomechanical Stability and Methane Emission in Longwall Mine Workings

R. Kamarov [1], Zh. Assanova [1*], Sh. Zeitinova [1*], Zh. Azimbayeva [1], J. Bogzhanova [1]

[1] *Abylkas Saginov Karaganda Technical University, Karaganda 100012, Kazakhstan.*

Received 23 September 2025; Revised 22 February 2026; Accepted 04 March 2026; Published 01 April 2026

Abstract

Under the conditions of the transition of the mines of the Karaganda Coal Basin to a high-productivity "mine–longwall" operating model, there is an increasing need to implement rational technologies for the development of mine workings that ensure higher drivage rates, reduced gas emission, and improved geomechanical stability of the rock mass. The purpose of this work is to study the influence of anchor support on the geomechanical and gas-dynamic state of the rock mass adjacent to the longwall mining area through a combination of field investigations and numerical flow modeling (ANSYS CFX), and to analyze the resulting properties of the side rocks and the stability of anchored mine workings. The research methodology included in situ observations under underground mining conditions, instrumental monitoring of roof displacement and rock stratification using KDM-1 and KDM-2 deformation control devices, analysis of outburst hazard indicators of the coal seam, and numerical simulation of methane distribution in mine workings using the Ansys CFX software package. The studies were carried out in development workings of the Kuzembayev Mine and the Saranskaya Mine at depths of 438–577 m. The results show that reducing the spacing between rock bolt rows to 0.5 m and increasing the bolt length to 2.4 m provides a reduction in vertical roof displacements to 5–30 mm and decreases absolute methane emission by 23%. The use of yielding rock bolt–frame support contributes to a reduction in the stress state of the rock mass, limits roof stratification, and eliminates manifestations of outburst hazard. The scientific novelty of the study lies in a comprehensive assessment of the relationship between rock bolt support parameters, the geomechanical condition of the rock mass, and gas emission, as well as in substantiating the effectiveness of yielding rock bolting systems in zones influenced by longwall mining under complex geological and mining conditions.

Keywords: Anchor Support; Stress-Strain State of Rock Mass; Mine; Mine Workings; Rock; Seam; Conveyor Passage; Ventilation Passage; Metal Arch Support; Absolute Gas Content.

1. Introduction

Currently, three main types of rock bolts are widely used in underground mining practice: mechanical bolts, fully grouted bolts with cementitious bonding agents, and fully grouted bolts with polymer (resin) bonding. Among these, fully resin-grouted bolts are the most commonly applied in the coal mines of the Karaganda Basin. Mechanical bolts, particularly expansion-shell bolts, are generally not used in coal mines, as their load-bearing capacity decreases over time due to roof sagging and relaxation of the expansion mechanism. The application of resin-grouted bolts in underground mining is constrained by the relatively high cost of polymer resins. However, their use is justified by their extremely short setting time and the ability to provide almost immediate support to freshly exposed roof strata, especially under weak, fractured, or water-bearing roof conditions. Fully cement-grouted bolts are comparatively inexpensive and, from a technical standpoint, are well suited for use in coal mine roadways.

* Corresponding author: zh.assanova@ktu.edu.kz; zeitinova_rmpi@mail.ru

https://doi.org/10.28991/CEJ-2026-012-04-013

Ongoing improvements in rock bolting technology are focused both on the development of bolt designs with enhanced reliability of fixation in boreholes and on the advancement of specialized equipment for drilling and bolt installation. In the United States, approximately 70% of installed rock bolts are used in combination with fast-setting synthetic (resin) grouts. The remaining 30% consist of purely mechanical bolts, although these are often supplemented with cementitious grouts or point-fixed resin cartridges. Typical bolt lengths range from 1.2 to 2.4 m, with diameters of 16–22 mm. It is estimated that approximately one million rock bolts are installed annually in underground mines worldwide, with about 88% of this total used in the United States [1].

In Australia, 34 out of 51 operating mines employ longwall mining systems, where panel development is carried out using paired roadways. The excavation of these roadways is one of the factors limiting the rate of panel preparation. In each roadway, six roof bolts are typically installed per row in the roof and one bolt in each sidewall at 1 m intervals as the heading advances [2].

In the United Kingdom, all 17 currently operating coal mines, as well as one mine in Scotland, utilize roof bolting as the primary support method during longwall panel development with single-entry roadways, leaving coal pillars between adjacent panels. In deep mines, additional roof reinforcement is often required under conditions of high in-situ stress or weak roof strata. For this purpose, high-strength rock bolts with a yield capacity of approximately 250 kN, installed with high-strength and high-stiffness resin grouts, have been developed for use in British mines. In high-capacity longwall faces operated under retreat (reverse) mining conditions, face advance rates typically reach 50–60 m per week [3–5].

At present, approximately 90% of development roadways in British retreat-mined panels are supported using rock bolts. At depths of 700–1200 m, the bolt density is significantly higher than that observed in other Western mining countries. Typically, 7–12 bolts with a length of 2.4 m are installed per meter of roadway, with an additional 1–2 bolts of 1.8 m length installed in the sidewalls. The implementation of systematic roof bolting has led to a substantial improvement in occupational safety. Injury rates during roadway development have decreased from 3.4 to 0.9 cases per 100,000 man-shifts, while material costs per meter of excavation have been reduced by approximately 50%.

In South African mines, where the room-and-pillar mining method predominates and coal production accounts for only about 10% of total output, self-propelled bolting machines are widely used. Despite generally favorable roof conditions, characterized predominantly by competent sandstone strata, considerable attention is paid to monitoring the condition of roof bolts and preventing localized roof falls in areas affected by geological disturbances.

In India, both point-anchored mechanical bolts and fully cement-grouted bolts are employed, providing load-bearing capacities of up to 60–80 kN. In the near future, the introduction of fully resin-grouted bolts is anticipated. In China, systematic roof bolting is currently applied mainly in large-scale mining operations [3]. In Poland, roof bolting has not been implemented on a systematic basis, primarily due to complex geological conditions and the operational strategy aimed at maximizing coal recovery through the reuse of development roadways when mining adjacent longwall panels.

In the coal industries of the United States, Australia, South Africa, the United Kingdom, and the Kuznetsk Coal Basin of the Russian Federation, the proportion of development roadways supported by rock bolts reaches 80–100%. The widespread application of rock bolting significantly reduces support costs compared to steel arch supports, increases roadway advance rates, and creates favorable conditions for achieving high production rates at longwall faces [4]. With proper selection of rock bolt support parameters, including bolt length, installation density, and pretension force, the safety of underground mining operations is substantially enhanced, and occurrences of roof falls and support failures are effectively minimized.

However, in the mines of the Russian Donbass, the application of advanced rock bolting systems in development roadways does not exceed 20–25% of the total roadway length. This limitation is attributed to complex geological, mining, and technical conditions, including the extensive reuse of roadways (approximately 90%) and the prevalence of difficult-to-cave main roof strata with layered or fractured immediate roof conditions in about 70% of development areas [5].

In the mines of the Russian Federation, roof falls, collapses, and failures of individual elements of rock bolt and supplemental supports in development roadways cannot be completely eliminated. The unsatisfactory condition of mine roadways necessitates labor-intensive and costly repair and rehabilitation operations, leading to reduced face productivity, deterioration of ventilation conditions, decreased operational safety, and, ultimately, unprofitable mine operation [6–8].

The primary causes of unsatisfactory roadway conditions include the following [9]:

- Insufficient initial pretension and load-bearing capacity, as well as significant non-uniform loading of individual bolts when using existing steel–polymer bolt systems (e.g., asp, a16v, a20v), resulting in bolt rod failure and deformation or rupture of 5 mm thick bearing plates;
- Insufficient strength of steel straps and mesh with thicknesses of 2–4 mm, leading to tearing or rupture;

- Low load-bearing capacity and floor penetration of existing supplementary supports, accompanied by their instability or failure;
- Excessive deformability and low load-bearing capacity of existing protective structures (timber cribs, stone pack walls, reinforced concrete and wood–concrete blocks, and cast phosphogypsum strips) in flooded deep roadways.

Considering these deficiencies, new types and parameters of rock bolt systems, supplementary reinforcement supports, and protective measures for development roadways under complex geological conditions have been tested in practice. These include high-strength steel–polymer bolts of the ASR1, ASG1, and ASG2 types, with lengths ranging from 2.0 to 4.2 m, load-bearing capacities of 190–350 kN, and yielding bearing plates activated at loads of 130–270 kN [2].

These bolts обеспечивают uniform load distribution on the bearing plate at deviations of up to 20° from the normal to the roof surface and generate an initial pretension force of 45–55 kN during installation, preventing delamination of the bolted roof strata [10]. For the reinforcement of low-height roadways, AK1 and AKSH1 cable bolts with load-bearing capacities of 175–260 kN have been developed. These bolts are used in combination with high-strength steel straps 6–8 mm thick and 120–150 mm wide, and, when necessary, with specially designed ZRO mesh ties and PZ support ties with a thickness of 8 mm and enhanced strength.

The load-bearing capacity of timber bolts with wedge locks ranges from 8 to 12 kN, depending on the wood species. Timber bolts are primarily used in short-term workings with a service life not exceeding 1.0–1.5 years, such as conveyor entries, ventilation roadways, crosscuts, and inclined workings in thick seams, as well as for reinforcing loose ground and longwall faces to prevent coal extrusion [11]. The load-bearing capacity of reinforced concrete bolts installed in rocks with a Protodyakonov strength coefficient f = 1–3 is 120–150 kN. The development of bolt anchorage strength over time is as follows: 15 kN after 30 minutes, 80 kN after 8 hours, and 120 kN after 5 days.

Polymer bolts are 4–5 times lighter than conventional steel bolts of the same length. Tests conducted in the Kuzbass, Lviv–Volyn, and Chelyabinsk coal basins have demonstrated positive results for polymer bolt systems. Rock bolt support systems are suitable for application under the following geological conditions [12]:

- Stratified rock masses with weakened interlayer bonding, where bolts integrate individual layers into a consolidated beam, significantly reducing crack development;
- The presence of weak immediate roof strata up to 1.5–2.0 m thick overlain by a competent main roof, where the weak roof is effectively suspended from the stronger overlying strata;
- Thick, slightly fractured, homogeneous rock masses, where bolting enhances interblock cohesion, increases rock strength and stability, and prevents the formation of a collapse arch;
- Weak and highly fractured rocks, where bolts are installed in combination with steel straps and mesh. Straps may be fabricated from flat steel, channels, special profiles, or welded round bars.

For short-term workings and in conjunction with timber bolts, wooden straps made from beams, planks, or sawn timber are also applied. A bolt installed with a fast-setting grout is considered point-anchored when the bolt rod is bonded within the borehole over a length of 0.6–0.8 m, while the bearing plate, tightened against the roof by a nut, transfers load to the bolt rod [13–17]. An increase in installation torque results in a higher clamping force exerted by the bearing plate on the roof strata. To reduce friction between the nut and the bearing plate, a polymer washer is used, enabling higher levels of bolt pretension. By combining different types of bolt anchorage, active roof control systems can be achieved. For example, a reinforced bolt rod and resin cartridges are installed in a drilled borehole, securing the bolt over a length of 1.0–1.2 m, while a high-strength steel extension rod is connected via a coupling to the bonded section. A bearing plate is then installed and tightened against the roof using a nut.

Such systems exhibit good compatibility with the rock mass reaction curve. In the mechanically anchored section, displacement, bending, and sliding may occur; however, overall roadway stability is maintained. Consequently, in underground mines, efforts are made to install rock bolt support as early as possible after excavation so that the bolt rods are mobilized during initial rock mass deformation.

Wang et al. [18] investigated the stability evolution of surrounding rock in underground roadways subjected to repeated mining disturbances. Their study demonstrated that multiple mining-induced loading cycles lead to cumulative stress redistribution, expansion of plastic zones, and progressive degradation of the bearing capacity of the surrounding rock mass. The authors showed that decreasing the spacing between adjacent mined seams significantly intensifies roof subsidence and lateral deformation of roadways. Their results confirm that rationally designed rock bolt systems can effectively suppress deformation of the roof and sidewalls by restraining crack propagation and limiting the development of plastic zones under repeated mining conditions.

Ren et al. [19] conducted a comprehensive investigation into the anchoring mechanism of rock bolts in cemented broken surrounding rock. By combining laboratory testing and numerical simulation, they analyzed the influence of bolt parameters on the formation of reinforced compression zones around excavations. Their results indicate that bolt density and installation pattern have the greatest impact on the mechanical performance of the anchored rock mass, while bolt length controls the axial range of reinforcement and bolt spacing determines its radial extent. The study also demonstrated that increasing bolt pretension significantly enhances the active support effect, improving the integrity and stability of fractured roof strata.

Dong et al. [20] focused on the real-time monitoring of rock bolt performance in underground mining roadways. They developed and implemented a monitoring system based on Fiber Bragg Grating (FBG) sensors embedded in rock bolts to measure axial force variations during mining operations. Field observations revealed that bolt loads increase sharply as the working face approaches, reflecting the dynamic response of the surrounding rock mass to mining-induced stress redistribution. Their work provides valuable insight into the load transfer mechanism between the rock mass and the support system and highlights the importance of continuous monitoring for early detection of abnormal bolt behavior.

Li et al. [21] explored advanced deformation monitoring techniques for assessing the stability of underground excavations. Their research demonstrated the applicability of ground-based synthetic aperture radar (GB-SAR) for high-resolution, non-contact monitoring of roof deformation in underground environments. The results showed that millimeter-scale displacements of the roof can be detected at an early stage, allowing timely evaluation of the effectiveness of support systems and early warning of potential instability. This approach offers significant advantages over traditional contact-based monitoring methods in harsh mining conditions.

Zhang et al. [22] investigated the deformation and failure mechanisms of heterogeneous rock masses under complex loading conditions through experimental and numerical analyses. Their findings emphasize that microstructural characteristics, including crack distribution, layering, and interfacial bonding, play a decisive role in controlling the mechanical response of the surrounding rock mass. The study highlights that these structural features directly influence the performance of anchorage systems and must be considered when designing support schemes for deep and complex mining environments.

Liu et al. [23] proposed an integrated geomechanical monitoring framework combining rock bolt force measurements, deformation monitoring, and numerical modeling. Their work demonstrates that coupling support performance data with rock mass deformation characteristics enables a more comprehensive assessment of roadway stability. The authors also emphasized the importance of linking mechanical deformation with changes in permeability and gas migration pathways, particularly in coal-bearing strata affected by mining-induced damage.

While anchor support technology is widely used in coal mining globally, and its basic mechanical effects and support principles have been extensively studied, most existing literature focuses on the influence of anchors on stress distribution in surrounding rock, deformation control, and the performance optimization of the support structures themselves. For high-gas, outburst-prone coal seams, there is a lack of systematic research combining in-situ measurements and numerical simulation to investigate the mechanism of anchor support's influence on gas migration dynamics and emission patterns in the surrounding rock mass. Particularly in mining regions with complex geological conditions, high gas content, and great depth like the Karaganda Basin, comprehensive studies on how anchor support affects gas drainage efficiency, changes in outburst hazard indicators, and the coupled relationship between fracture evolution in the surrounding rock and gas behavior remain a significant gap.

This study addresses this gap by employing a combined approach of field industrial trials (e.g., in the 42k10-z conveyor tunnel) and numerical modeling (using ANSYS CFX). It systematically analyzes the impact of anchor support parameters (such as bolt spacing, length, and yielding node presence) on surrounding rock deformation, absolute gas emission rates, and outburst hazard indices. Furthermore, it proposes an optimized anchor support scheme for roadways in high-gas coal seams. The results not only confirm the effectiveness of anchor support in controlling rock deformation but also reveal, for the first time in this region, the mechanism by which anchor support reduces absolute gas emission and enhances gas drainage effectiveness. This provides new technical rationale and design references for the safe and efficient mining of similar geological conditions.

To achieve these goals, this research employs a combined methodological approach. Field observations and monitoring of rock deformation and gas emissions in instrumented mine workings provide empirical data on the performance of anchor support. This is complemented by numerical simulation using the ANSYS CFX software package to model gas flow dynamics and concentration distributions under different support schemes, offering a deeper analytical insight into the coupled geomechanical and gas-state changes.

2. Problem Solution

2.1. Study of the Influence of Anchoring on the Geomechanical and Gas State of the Adjacent Rock Mass

Due to the ongoing transition of mines in the Karaganda coal basin to the "mine–longwall" operational model and the preparation of high-productivity longwalls, there is an increasing need to delineate mining blocks with sufficiently large coal reserves and to drive mine workings equipped with optimally designed support systems that ensure minimal time expenditure during final operations. The development and implementation of advanced anchor support technologies for mine workings have made it possible to significantly enhance operational safety during the installation of support systems, as well as to reduce injury rates during extraction operations at the final stage of mining. This is primarily achieved by preventing stratification and delamination of the roof rocks. For a period of three years, preparatory work has been conducted at the Kuzembaev Mine on the western wing to facilitate the development of coal seams k10 and k12, with total geological reserves amounting to 8.2 million tonnes of coal [24].

Mining operations are carried out below the +150 m level in an area classified as hazardous with respect to sudden coal and gas outbursts, at depths ranging from 438 to 577 m. Over a period of 19 months, from April 1999 to October 2000, conveyor and ventilation inclines 40k10-z with a total length of 1,060 m were driven. The inclines were excavated using a GPKs roadheader with a cross-sectional area of 10.3 m². The mine workings were supported by KMP-3A steel arch supports (Figure 1).

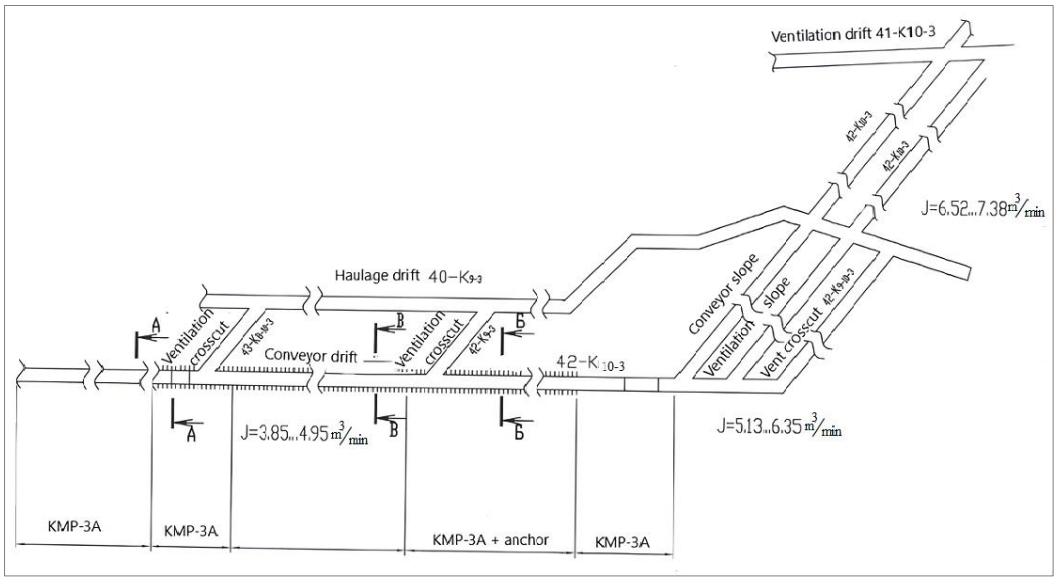

Figure 1. Schematic diagram of conveyor tunnel 42k10–3: a – arch support with anchors; b – semi-arch support with anchors; c – trapezoidal support with anchors

Due to the high gas content of the rock mass (6.52–7.38 m³/min), the inclines were driven sequentially in 200 m sections, which were interconnected by crosscut tunnels. Ventilation of the working faces was provided by VMC-8 auxiliary fans and two ventilation shafts supplying an air flow rate of up to 715–929 m³/min.

During the development of the workings using the current forecasting method, 19 zones were identified as outburst-hazardous (OZ) with respect to sudden coal and gas emissions. In accordance with the approved "Passport for Mining Operations," a comprehensive set of anti-outburst measures was implemented, including the drilling of advance relief boreholes, exploration boreholes, and lateral degassing boreholes. Over the specified period, a total of 692 boreholes with an aggregate length of 18,639 m were drilled. Owing to the large volume of drilling operations, the high gas content, and the frequent occurrence of hazardous sudden coal and gas emissions, the average drilling advance rate did not exceed 40–60 m per month [24, 25].

In order to reduce the time required for the preparation of the 42k10-z longwall, with recoverable reserves of 1.6 million tonnes of coal, the mine adopted a field development scheme. This involved driving mine workings along the k9 seam, with a thickness of 0.6 m, followed by their connection to the 42k10-z conveyor roadway by means of ventilation crosscuts. The 40k9-z haulage drift was excavated using a KSP-32 roadheader with a cross-sectional area of 14.4 m², achieving an advance rate of 240–477 m per month.

Between May and November 2003, the 42k10-z conveyor roadway was driven. During this period, a total length of 1,030 m was excavated, with a cross-sectional area ranging from 12.8 to 14.4 m². Over a length of 160 m, the roadway was supported by KMP-3A steel arch supports. At intervals of 15 m, and subsequently every 60 m of advance from the reference point, the coal and gas outburst hazard indices were determined using the current forecasting method.

Accordingly, excavation was conducted in compliance with the requirements of the "Passport for Mining Operations," including the drilling of advance relief and lateral degassing boreholes. In order to increase the drilling rate and reduce the unit cost of roadway excavation, a transition was made to a combined frame-and-anchor support system, with a frame spacing of 1.0 m and a distance between anchor rows of 0.8–0.9 m (Figure 2).

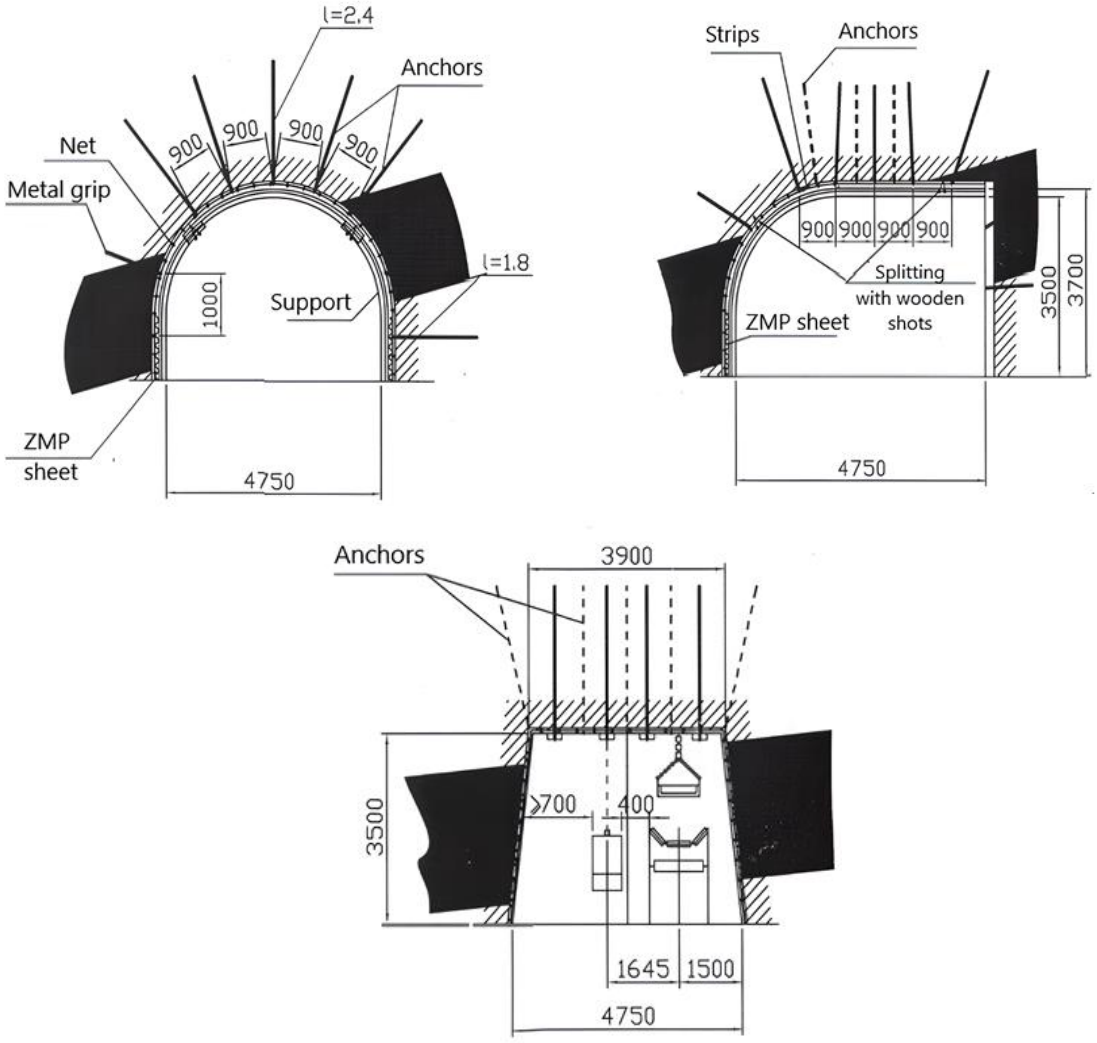

Figure 2. Technological diagram of the 42k10-z conveyor tunnel fastening: a – arch fastening with anchors; b – semi-arch fastening with anchors; c – trapezoidal fastening with anchors

The installation of the frame-and-anchor support system was carried out in the following sequence. After cutting the rock mass to the planned advance length, boreholes were drilled using a Super-Turbo drilling rig. Owing to its relatively compact dimensions (1700–4600 mm) and low weight (45 kg), this rig enables the drilling and installation of a 2.4 m long KA-1-03 steel anchor, fixed using four KAKS-P polymer resin cartridges, within approximately 4 minutes. Consequently, securing the face for an advance of 0.7–0.8 m required 20–30 minutes, after which a KMP-3A frame, or another frame modification, was installed, followed by the drilling and installation of side anchors [26]. After the excavation of 90 m, the support design parameters were revised. Subsequent drivage over a distance of 165 m was performed using special steel anchors, with the spacing between anchor rows reduced to 0.5 m (Figure 2, Section B–B).

With further advancement to PC 41, the support passport was revised once again. During subsequent excavation over a length of 310 m, the roadway cross-section adopted a trapezoidal shape combined with anchor support, maintaining a spacing of 0.5 m between anchor rows (Figure 2, Section B–B). A straight steel profile was fixed to the roof of the roadway by four anchors, each 2.4 m in length. Between the profiles, steel straps were installed at 0.5 m intervals, accompanied by the drilling and installation of five anchors at each interval. The sidewalls of the roadway were reinforced using 1.8 m long anchors, at a density of four anchors per running meter.

To determine control displacements of the roadway roof, leveling measurements were conducted every 10 m along contour benchmarks. Based on observation results obtained twice monthly between June 17, 2003, and January 16, 2004, the maximum vertical displacements of the roof rocks ranged from 71 to 78 mm in the station 26–30 zone (Figure 3) [27].

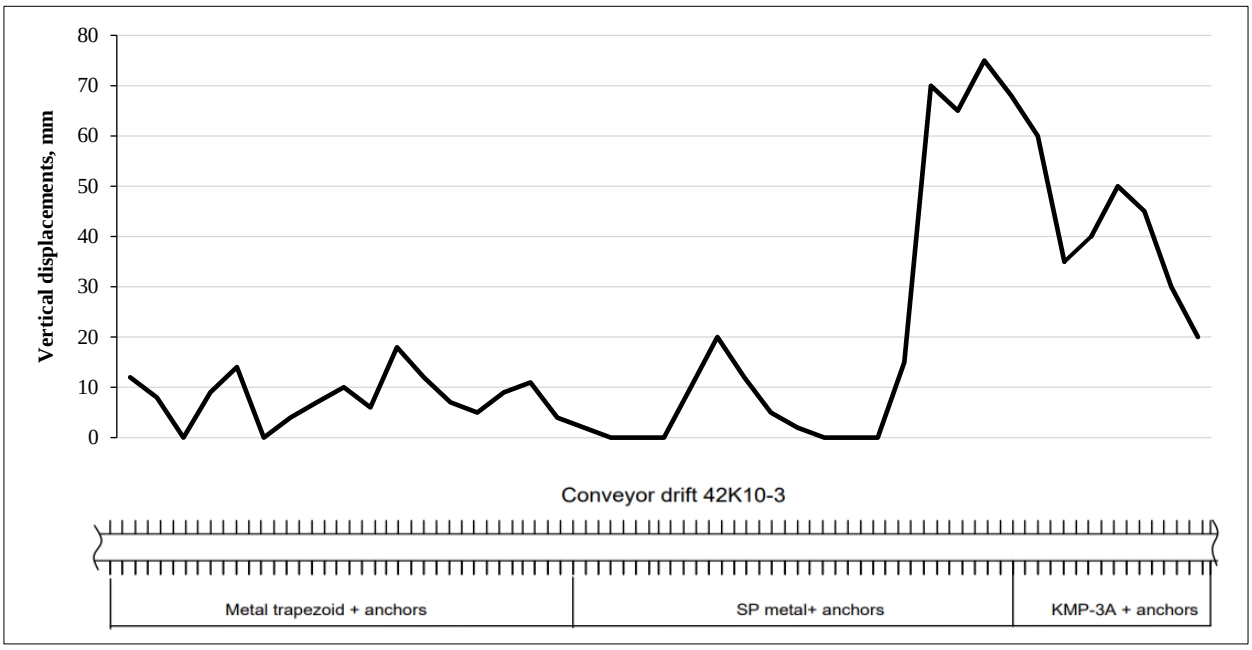

Figure 3. Vertical displacement of the roof rock in conveyor tunnel 42k10-z: station – 41 – 65 – trapezoidal fastening with anchors; station - 27 – 41 - semi-arch fastening with anchors; station – 16 – 27 – arch fastening with anchors

A summary of the key operational parameters, support configurations, and corresponding results for the different sections of the 42k10-z conveyor tunnel is provided in Table 1. The data clearly illustrates the progression from traditional arch support to optimized combined anchor support and its measurable impact on roof displacement and gas emission control.

Table 1. Summary of key parameters and results from field investigations in the 42k10-z conveyor tunnel

Parameter / Condition	Section A (Initial Drive)	Section B (Revised Support)	Section C (Optimized Support)	Notes / Source
Location / Mine	Kuzembaev Mine	Kuzembaev Mine	Kuzembaev Mine	Western wing
Seam	k10	k10	k10	-
Approx. Depth (m)	438 - 577	438 - 577	438 - 577	Below +150 m level
Tunnel Section (m²)	12.8 – 14.4	12.8 – 14.4	12.8 – 14.4	-
Primary Support Type	Metal Arch (KMP-3A)	Combined Frame-Anchor	Trapezoidal + Anchor	Figure 2
Anchor Type	Not Applied	KA-1-03 Metal Anchor	KA-1-03 Metal Anchor	+ KAKS-P ampoules
Anchor Length (m)	–	2.4	2.4	-
Distance Between Anchor Rows (m)	–	0.8 – 0.9	0.5	-
Roof Anchors per Row	–	4	5	With strip support
Side Anchor Length (m) / Density	–	1.8 / 4 per m	1.8 / 4 per m	-
Max. Vertical Roof Displacement (mm)	71 – 78	-	5 – 30	Figure 3
Absolute Gas Emission (m³/min)	5.13 – 6.35	3.85 – 4.95	3.85 – 4.95	At the face
Avg. Initial Gas Emission Rate (l/min) *	10.2 – 8.5	4.2 – 7.0	4.2 – 7.0	1st two intervals
Outburst Hazard (OZ) Detected	Yes (1-2)	No	No	-
Key Outcome	Baseline for comparison	Improved stability & gas control	Optimal performance achieved	-

* Measured in control boreholes at one-meter intervals.

Reducing the spacing between anchor rows to 0.5 m and increasing the anchor length to 2.4 m resulted in a stable reduction of vertical roof displacements to 5–30 mm. The decrease in vertical displacement of the roof rocks led to a reduction in methane emission from the adjacent rock mass, which, in turn, reduced the absolute gas emission by 23%, corresponding to 1.5 m³/min. Whereas the absolute gas emission at the face during the first 160 m of drivage supported by steel arch frames amounted to 5.13–6.35 m³/min, after the transition to anchor support the absolute gas emission decreased to 3.85–4.95 m³/min when mining at the same elevation. For comparison, the absolute gas emission in previously driven inclines supported by frame support was 6.52–7.38 m³/min.

The change in the roadway support technology through the implementation of anchor support made it possible to abandon the previously applied lateral degassing measures. Moreover, over a drivage length of 600 m, no hazardous values of the outburst hazard index were recorded, despite the fact that excavation was conducted within the zone of increased geodynamic disturbance (PGD) associated with previously mined seams k13–k14.

When applying the current forecasting method for outburst hazard in workings supported by steel arch frames, hazardous values (OZ) were identified in one to two intervals of the control boreholes due to high gas emission rates and the stressed state of the rock mass. Following the transition to anchor support, a reduction in gas emission intensity was observed in the first two to three intervals of the control boreholes, which resulted in a corresponding decrease in the degree of outburst hazard.

During the excavation of roadways supported by steel arch frames, the average initial gas emission rates in the first two control intervals ranged from 10.2 to 8.5 L/min. In contrast, when driving the conveyor roadway with anchor support, the average initial gas emission rates in the first two control intervals were reduced to 4.2–7.0 L/min.

2.2. Gas Measurement Methodology and Calibration

The measurement of methane emission was conducted in strict accordance with the mine's operational safety protocol. The initial gas release rate (l/min) from control boreholes was measured using calibrated catalytic combustion (pellistor) methanometers (e.g., SG-3 or equivalent certified detectors), following a standardized stabilization period after drilling. Absolute gas emission (m^3/min) into the ventilation stream was calculated based on continuous measurements of airflow velocity (using calibrated anemometers) and methane concentration differentials across the working face. All instruments underwent routine pre-shift calibration with certified standard gas mixtures, and reported volumes were corrected to normal conditions (101.325 kPa, 20°C). This consistent measurement and calibration protocol across all excavation stages ensures the comparability of gas emission data between the different support schemes.

The absence of dangerous values of the emission hazard index is explained by a decrease in the reference pressure at the face and a decrease in gas release from the seam due to a reduction in the stratification of the roof rock (Figure 4) [28].

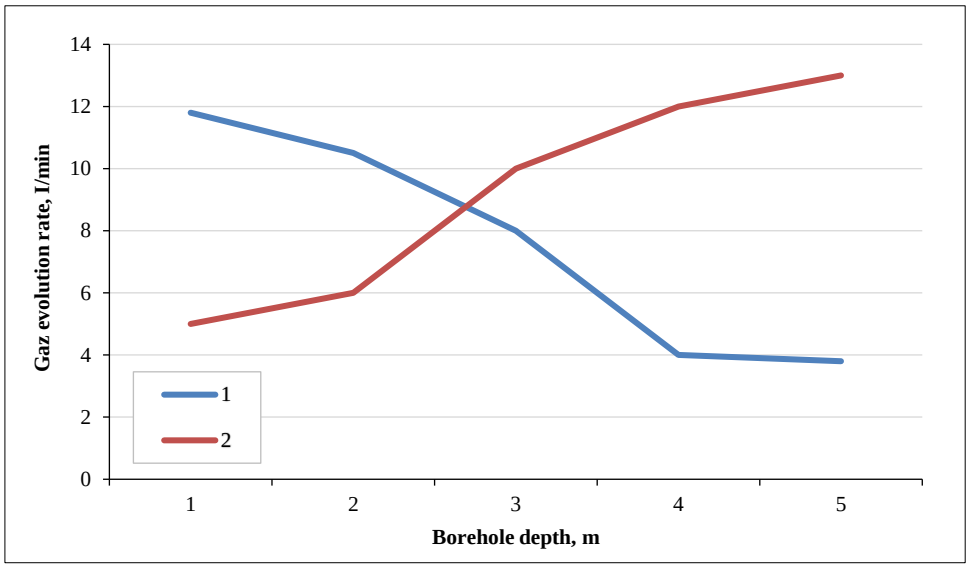

Figure 4. Actual data on the average initial gas release rate for control boreholes at one-meter intervals: 1 – arch support, 2 – anchor support (the figure shows the average gas release rates during the excavation of the 42k10–z conveyor tunnel along its entire length).

Use of anchor bolts to secure the 42k10-z conveyor tunnel allowed for an increase in tunneling speed to 140-160 m per month. The use of anchor fastenings during the construction of the 42k10-z conveyor tunnel led to a reduction in absolute gas emissions in the workings, the elimination of dangerous levels of gas emissions from the seam, a significant reduction in the volume of drilling work, and a reduction in the labor intensity and costs of tunneling [17].

3. Results and Discussion

3.1. Assessment of Data Variability and Uncertainty

The quantitative results presented, such as roof displacements (5–30 mm) and gas emission rates (e.g., 3.85–4.95 m^3/min), are reported as observed ranges from field measurements. These ranges inherently capture some of the operational variability experienced during tunneling. However, providing statistical measures of uncertainty (e.g., standard deviations, confidence intervals) would offer a more rigorous assessment of the significance of the differences between support types.

For Displacement Data: The values presented (e.g., 71–78 mm for arch support vs. 5–30 mm for anchor support) represent the observed maximum vertical displacements at specific monitoring stations over time (Figure 3). A more complete statistical treatment would require multiple, simultaneous displacement measurements at each support configuration to calculate mean displacement and standard deviation for each scheme.

For Gas Emission Data: The gas release rates (l/min) from control boreholes and the calculated absolute emissions (m^3/min) are single measurements per interval or averaged over a tunnel section. The reported ranges (e.g., 10.2–8.5 l/min vs. 4.2–7.0 l/min) stem from measurements taken at different locations/times under each support regime. To statistically validate the reduction, one would need repeated measurements under similar conditions to establish a variance.

Interpretation and Forward Look: While the current data format (presented ranges) is common in initial field studies and clearly shows a strong, favorable trend for anchor support, future research should incorporate a designed sampling plan to collect replicate data. This would allow for proper statistical hypothesis testing (e.g., t-tests) to confirm the significance of the observed reductions in displacement and gas emission with a defined level of confidence. The numerical modeling results (Section 2.3), which show a consistent 23% reduction in a controlled simulation, provide strong complementary, deterministic support for the field-observed trend.

3.2. Consideration of Confounding Factors and Validity of Comparison

While the data demonstrate a clear correlation between the implementation of anchor support and improved geomechanical and gas-dynamic outcomes, it is important to consider potential confounding factors to validate a causal relationship. The primary challenge in this field study is that the comparison is made across sequential stages of advancing the same tunnel, rather than through simultaneous, controlled experiments.

The following factors were identified and their potential influence assessed:

- ***Temporal and Sequential Execution:*** The tunnel sections with arch support were excavated earlier (May-November 2003) than the sections with optimized anchor support. While this sequence could introduce time-dependent variables, key constant factors mitigate this
- ***Seam and Depth:*** All excavations occurred in the same k10 seam and within the same depth range (438–577 m), ensuring comparable baseline geomechanical and gas conditions.
- ***Outburst Hazard Protocol:*** The same strict forecast method and mitigation measures (e.g., advance drilling) were applied throughout, as mandated by the operational "Passport."
- ***Evolution of Support Design:*** The anchor support itself was not a single, fixed variable. Parameters were optimized during the drive (e.g., row spacing reduced from 0.8 m to 0.5 m). The observed improvements correlate with this progressive optimization, strengthening the argument that the anchor system's specific configuration is a decisive factor.
- ***Change in Cross-Section Geometry:*** The support change coincided with a shift from an arched to a trapezoidal profile. While the geometry influences stress distribution, the primary mechanism for gas reduction cited - the reduction of roof stratification and displacement—is directly attributable to the action of the anchors in binding rock layers, not the profile shape. The trapezoidal section with anchors performed better than the earlier arched section with anchors, further pointing to the role of support density.
- ***Potential Geological Variability:*** Although the tunnel advanced through the same seam, local heterogeneity in roof rock strength or fracturing is possible. However, the continuous nature of the measurements (vertical displacement, gas emission rates) shows a trend that aligns precisely with support changes, not with random fluctuations. The most significant improvement occurred after a deliberate, engineered change (reduced anchor spacing), not at an arbitrary location.
- ***Conclusion on Validity:*** Although a perfectly controlled experiment is unattainable in a mining environment, the evidence strongly suggests that the anchor support is the principal cause of the observed improvements. The consistency of the geological setting, the continued application of gas control protocols, and the direct temporal correlation between specific engineering interventions (increased anchor length and density) and measurable improvements in stability and gas emission provide a robust, cause-effect rationale. The numerical modeling (Section 2.3) further supports this by isolating the support type as a variable in a controlled simulation, confirming the field-observed trend.

3.3. Study of Side Rock Properties and Geomechanical Conditions of Anchored Mine Workings

At the Saranskaya Mine of ArcelorMittal Temirtau, studies were conducted on the stability and caving behaviour of roof and sidewall rock masses reinforced with rock bolts, as well as on their stratification, deformation, and displacement characteristics. Determination of the initial rock stratification zone makes it possible to predict the stability and potential collapse of the roof and sidewalls of mine workings, thereby enabling the selection of rational support design parameters.

To identify rock stratification, remote monitoring of the stress–strain state (SSS) of the rock mass, roof failure processes, and sidewall displacements was carried out using DMS-1 and DMS-2 rock mass deformation monitoring devices. During operation of the DMS-1 device, the occurrence of rock failure, as determined by the sensor settings, causes the light-emitting indicators to switch from green to red, thereby providing visual monitoring of stratification within the rock mass. When using the DMS-1 device, the magnitude of rock mass displacement is determined by the number of consecutively illuminated segments on the electronic indicator, which provides a quantitative assessment of roof rock delamination (Figure 5).

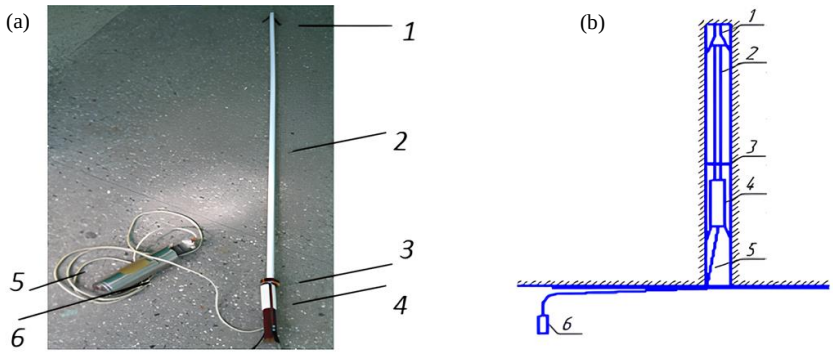

Figure 5. General view (a) and measurement diagram (b) using DMS-1 and 2 deformation monitoring devices: 1, 2 – base reference point and its rod; 3 – thrust washer; 4 – sensor; 5 – connecting cable; 6 – DMS-2 device

Displacements of the surrounding rock mass were measured in the 71k10-B conveyor roadway at the Saranskaya Mine of ArcelorMittal Temirtau JSC at a depth of 450 m. To monitor rock mass movements, three boreholes were drilled in the roof of the roadway: one central borehole and two boreholes inclined at an angle of 45° to the central one. The immediate roof of the seam is composed of moderately stable argillites with a thickness of up to 5 m, a compressive strength of 10–20 MPa, and a joint spacing of approximately 0.5 m. Above this lies the main, difficult-to-cave roof, with a thickness of 24–30 m, composed of sandstone with a compressive strength of 45–80 MPa [29].

The principle of controlling roadway stability based on the self-unloading and self-stabilization of the surrounding rock mass, regulated by a flexible anchor support system, was tested under these conditions. During anchor operation, the spacer element ensures anchor flexibility, which allows this support system to be applied in complex mining and geological conditions, including those with difficult-to-control roofs, such as those characteristic of the strata at the Saranskaya Mine of ArcelorMittal Temirtau JSC.

An experiment aimed at increasing anchor flexibility was conducted in the 71k10-B conveyor roadway over a length of 5 m. In accordance with the repair and rehabilitation project for the main return crosscut of the fourth horizon, steel tubes were installed between the anchor hook and the bearing plate. The tubes had an outer diameter of 0.03 m, a wall thickness of 0.0015 m, and a height of 0.07 m. The roadway was supported by anchors 2.4 m in length and 0.022 m in diameter, installed using four KAKS-P resin cartridges. During the observation period, deformation of the tubes in the form of compression of 3–5 mm was recorded. Subsequent inspections revealed further deformation, with the tubes compressed almost to the thickness of the bearing plate (Figure 6).

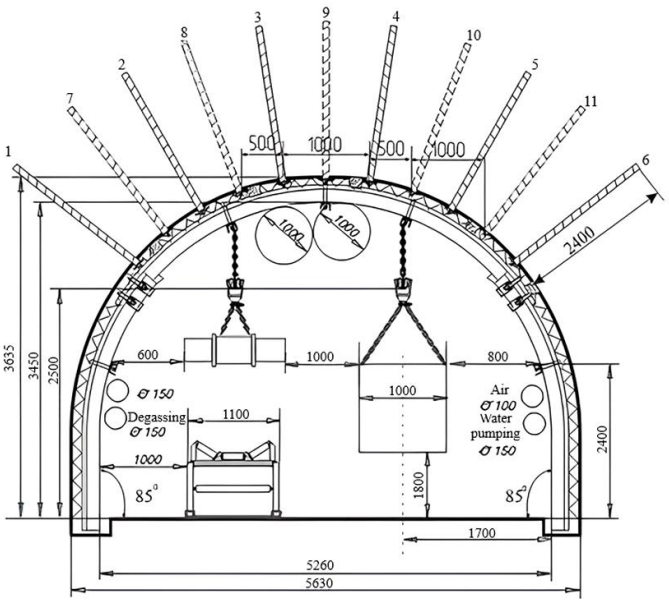

Figure 6. Experimental studies of anchor ductility at the Saranskaya mine of ArcelorMittal Temirtau JSC

The roof reinforced with a combined flexible anchor–frame support system operates in three distinct stages: a rigid operating mode, a flexible mode accompanied by stratification and displacement of rock layers, and a long-term stability mode characterized by sustained load-bearing capacity due to the combined action of anchor and frame supports and the self-locking of rock blocks. Under rigid support conditions, an increase in load results in a proportional increase in shear stresses, whereas under flexible support conditions, shear stresses remain relatively stable.

Displacements observed with the flexible anchor–frame support system reached up to 0.3 m in the roof and 0.05–0.10 m in the sidewalls, while the activation value of the flexibility unit did not exceed 0.07–0.10 m. The crack development zone extended to depths of 0.5–0.9 m in the sidewalls and 2.4–3.0 m in the roof. These values are approximately 1.5 times lower than those obtained when using conventional metal frame support (MFS).

In the mentioned mine for comparison, we also investigated the modes of operation of combined metal frame bracing (MFB) with standard and limited-pliable anchors (Table 2) in the zone of influence of mining operations.

Table 2. Stability of contours of conveyor drift 71k10-B of mine "Saranskaya" UD JSC "ArcelorMittal Temirtau" depending on the technological parameters of anchoring

An. kN	Tc	La. m	Du. anchor/m²	Pc. kPa	Sk. mm	Pm. m	Uk
			Non-Flexible Anchors				
12	1	1.8	1.0	70	590	0.9	0.1
12	1	2.0	0.93	100	540	0.91	0.1
12	1	2.2	1.2	155	460	0.92	0.5
12	1	2.0	0.9	170	435	0.93	0.6
12	2	2.2	1.2	190	390	0.95	0.85
			Limited-Flex Anchors				
15	1	2.2	1.28	235	350	0.4	0.9
15	1	2.4	1.2	275	300	0.4	0.91
15	2	2.4	1.28	295	295	0.38	0.92
15	2	2.4	1.28	240	285	0.35	0.93
15	2	2.4	1.28	375	260	0.3	0.95

Note: An, is the load-bearing capacity of the anchor support, kN; Tc, is the number of reinforcement rows from the repair area; La, is the anchor length, m; Du, is the anchor installation density, anchors/m²; Pc, is the total resistance of the frame, anchor, and reinforcement support system, kPa; Sk, is the roof displacement, mm; Pm, is the degree of rock mass stratification within the anchor support installation zone, m; and Uk, is the stability coefficient of the roadway contour.

Reinforcement supports consisting of one to two rows of wedge props or hydraulic props installed beneath two rows of steel profiles were mounted directly at the face within the bearing pressure zone. Under these conditions, an increase in the design resistance of the anchor support, achieved through the introduction of a yielding (pliable) node, from 60 to 140 kPa (kN/m²) made it possible to reduce roof rock displacements from 60 to 25 mm, that is, by a factor of 2.35. When the number of delaminated contacts in weak rock layers is small (up to three layers), satisfactory roof conditions can be ensured by providing a design anchor resistance of 140–200 kPa with anchor lengths of up to 2.4 m. A further increase in anchor length or installation density under such conditions is technically and economically unjustified, as it does not result in a significant reduction in roof displacement or improvement of roof conditions, but only leads to a decrease in the advance rate of mining operations.

The application of deep-embedded yielding anchor–frame support enables its effective performance, including within zones influenced by longwall mining, while maintaining roadway stability without the need for repair. The load-bearing capacity of the yielding node varies within the range of 40–60 kN, and the yielding anchor–frame support system is capable of absorbing loads from 290 to 350 kN during the transition from the yielding to the rigid operating mode [30]. The use of frame anchors under conditions of significant stratification, rock mass displacement, and dynamic manifestations of bearing pressure allows a reduction in loads through their combined interaction with the surrounding contour rock mass.

3.4. Numerical Modeling of Methane Content Mine Excavation

In order to perform numerical simulation of gas emission processes in mine workings, the ANSYS CFX software package was selected due to a number of objective advantages.

- High accuracy of finite element computations. ANSYS CFX provides the capability to conduct advanced engineering analyses with a high degree of accuracy, which is particularly important when modeling stress–strain conditions and gas flow distribution within a heterogeneous geological medium.
- Capability to model multicomponent and multi-zone media. The software enables simulation of interactions between solid bodies, including the rock mass and support structures, and gaseous environments, while accounting for variable material properties and complex geometric configurations.

- User-oriented interface and modular structure. ANSYS CFX is equipped with integrated tools for geometric modeling, specification of boundary and initial conditions, mesh generation, and post-processing of numerical results.
- Advanced visualization capabilities. Owing to its extensive visualization functionality, ANSYS CFX allows clear representation of parameter distributions, such as methane concentration, across both cross-sectional planes and three-dimensional domains, thereby facilitating analysis and interpretation of the simulation results.

Figure 7 presents a block diagram of the numerical simulation algorithm, illustrating the logical sequence of the main stages, from the definition of geometry and boundary conditions to the acquisition and interpretation of the final results.

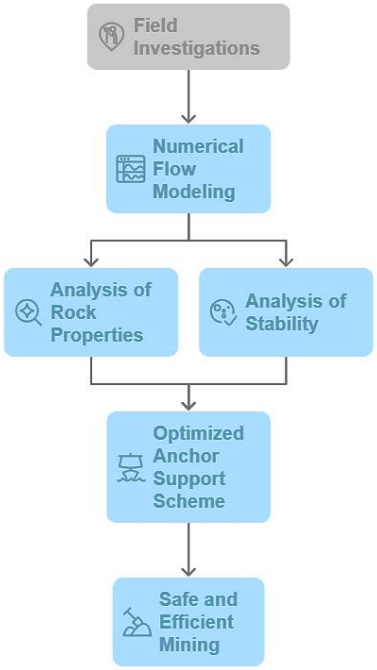

Figure 7. Block Diagram of the Numerical Simulation Algorithm

Furthermore, Figure 8 presents the mathematical model of a mine roadway supported by steel arch frames. The model illustrates the spatial distribution of gas within different zones of the surrounding rock mass. The color scale indicates gas concentration as follows: blue corresponds to areas with low or negligible gas content; green and yellow denote regions characterized by moderate gas emission intensity; and red, if present, would indicate zones of elevated gas concentration.

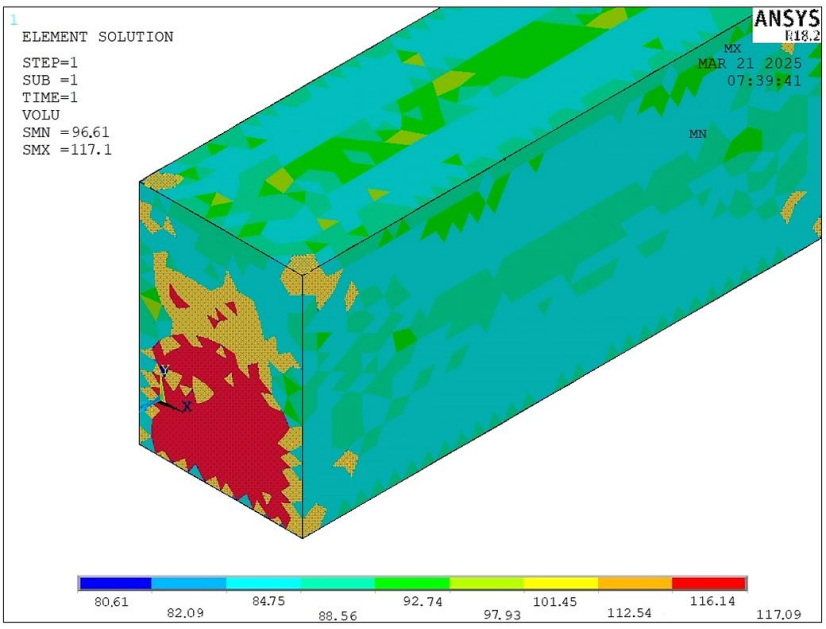

Figure 8. Excavation with arch support

Analysis of the simulation results shows that the minimum value of absolute gas emission is 80.61 m³/h, whereas the maximum methane emission within the roadway zone reaches 117.09 m³/h.

To provide a more comprehensive assessment, an additional numerical model was developed that incorporates a combined support system consisting of rock bolts in conjunction with steel arch support (Figure 9). Although visualization of this model was complicated by the high mesh density and the geometric complexity of the computational domain, the numerical calculations yielded reliable quantitative results, thereby enabling further interpretation and comparative analysis.

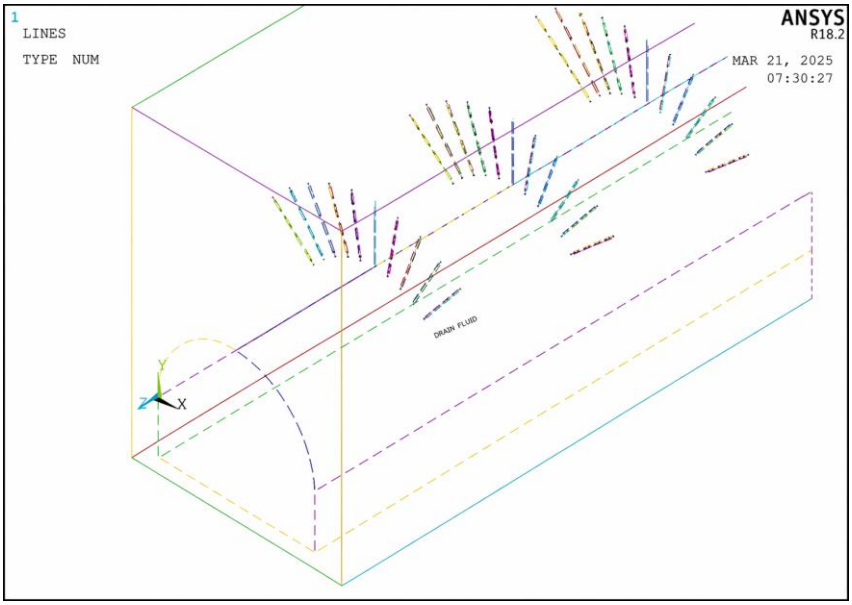

Figure 9. Mining excavation with combined fastening

Figure 10 shows a three-dimensional numerical model of the excavation with a combined support system. In this case, the maximum gas emission rate reaches 90.49 m³/h, which is 23% lower compared to the use of arch support alone.

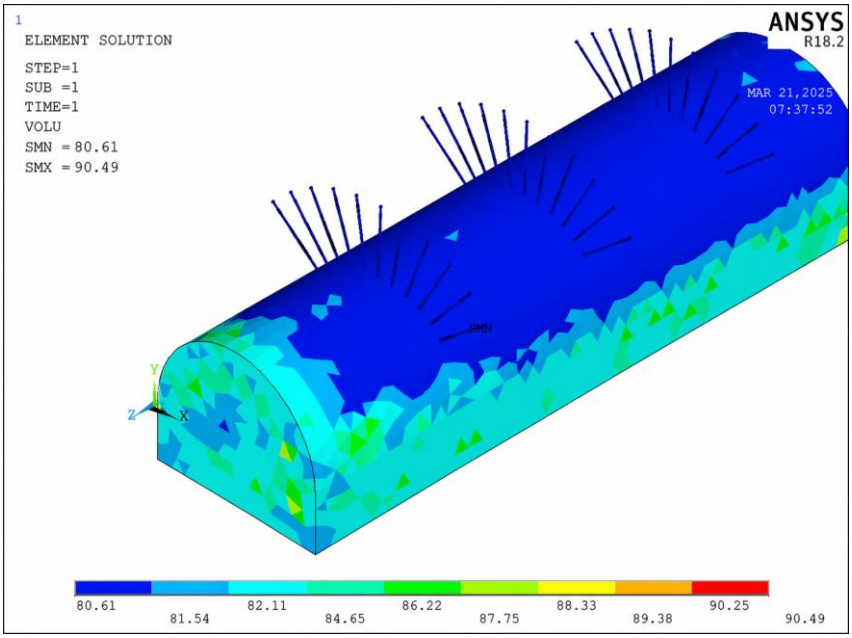

Figure 10. Three-dimensional numerical model of the excavation

The simulation results demonstrate that the application of combined support significantly reduces the intensity of gas emission in the mine roadway, which represents an important factor in improving both safety and the effectiveness of degasification measures. The choice of ANSYS CFX proved to be well justified, owing to its computational accuracy, flexibility in model configuration, and convenience in results analysis.

4. Conclusion

The conducted studies have demonstrated that the application of rock bolting and combined steel arch–rock bolt support in development workings of the coal mines of the Karaganda Basin is an effective technical solution that enhances the stability of mine workings, reduces gas emission, and increases drivage rates. It has been established that conventional steel arch support at significant depths and under conditions of high gas emission is associated with increased vertical roof displacements, rock stratification, and a higher level of outburst hazard. Experimental results confirm that reducing the spacing between rock bolt rows to 0.5 m and increasing bolt length to 2.4 m leads to a decrease in vertical roof displacements to 5–30 mm, which is 1.5–2 times lower than that observed with frame support. Stabilization of the surrounding rock mass results in reduced gas release from the coal seam and an average decrease in absolute methane emission into the workings by 23%. At the same time, the initial methane emission rate measured in control boreholes decreases by more than two times, which makes it possible to eliminate dangerous values of outburst hazard indicators even in zones affected by previously mined seams. Investigations of the geomechanical behavior of workings supported by yielding rock bolt–frame systems have shown that the presence of a yielding element ensures redistribution of rock pressure, reduces the load on the support, and prevents failure of the immediate roof. Increasing the design resistance of the rock bolt support from 60 to 140 kPa reduces roof displacements from 60 to 25 mm, confirming the high efficiency of yielding rock bolting systems. Numerical modeling using Ansys CFX further confirmed a reduction in maximum gas emission levels when combined support is applied.

Thus, the use of rock bolting and yielding combined support provides an integrated improvement of geomechanical and gas conditions, reduces labor intensity and development costs, and can be recommended for widespread implementation in the preparation of high-productivity longwalls in the Karaganda Coal Basin.

5. Declarations

5.1. Author Contributions

Conceptualization, K.R. and A.Zh.; methodology, K.R. and Z.Sh.; software, A.Zh.; formal analysis, A.Zh. and B.J.; investigation, K.R. and A.Zh.; resources, Az.Zh. and Z.Sh.; data curation, K.R. and B.J.; writing—original draft preparation, K.R.; writing—review and editing, Sh.Z.; visualization, Z.Sh. and A.Zh.; supervision, K.R. and Az.Zh.; project administration, K.R. All authors have read and agreed to the published version of the manuscript.

5.2. Data Availability Statement

The data presented in this study are available on request from the corresponding author.

5.3. Funding

The authors received no financial support for the research, authorship, and/or publication of this article.

5.4. Conflicts of Interest

The authors declare no conflict of interest.

6. References

[1] Demin, V., Kalinin, A., Baimuldin, M., Tomilov, A., Smagulova, A., Mutovina, N., Shokarev, D., Aliev, S., Akpanbayeva, A., & Demina, T. (2024). Developing a Technology for Driving Mine Workings with Combined Support and Friction Anchors in Ore Mines. Applied Sciences (Switzerland), 14(22), 10344. doi:10.3390/app142210344.

[2] Xie, H. (2017). Research Framework and Anticipated Results of Deep Rock Mechanics and Mining Theory. Gongcheng Kexue Yu Jishu/Advanced Engineering Sciences, 49(2), 1–16. doi:10.15961/j.jsuese.201700025.

[3] Zhang, T., Wu, J., Chen, Y., Ding, H., Ma, H., & Feng, R. (2021). The Relationship between Mining-Induced Stress and Coal Gas under an Optimized Support Scheme: A Case Study in the Guanyinshan Coal Mine, China. Geofluids, 2021(1), 1–17. doi:10.1155/2021/2421398.

[4] Wang, J., Wang, F., & Zheng, X. (2022). Stress Evolution Mechanism and Control Technology for Reversing Mining and Excavation under Mining-Induced Dynamic Pressure in Deep Mine. Geofluids, 2022. doi:10.1155/2022/4133529.

[5] Li, L., Kong, X. S., Yang, W., Huang, J. W., & Wang, Z. E. (2023). A Study of Anchor Cable and C-Shaped Tube Support for the Roadway of Shuangliu Coal Mine. Symmetry, 15(9), 1757. doi:10.3390/sym15091757.

[6] Šňupárek, R., & Konečný, P. (2010). Stability of roadways in coalmines alias rock mechanics in practice. Journal of Rock Mechanics and Geotechnical Engineering, 2(3), 281–288. doi:10.3724/sp.j.1235.2010.00281.

[7] Zheng, B., Bayat, M., Shi, Y., Cao, M., Jiang, Y., Qian, X., & Sumarac, D. (2025). A prognostic model of side friction of rock bolt anchoring section based on associated flow law. Kuwait Journal of Science, 52(2), 100374. doi:10.1016/j.kjs.2025.100374.

[8] Guo, X., Zheng, X., Li, P., Lian, R., Liu, C., Shahani, N. M., Wang, C., Li, B., Xu, W., & Lai, G. (2021). Full-stress anchoring technology and application of bolts in the coal roadway. Energies, 14(22), 7475. doi:10.3390/en14227475.

[9] Usenbekov, M. S., Isabek, T. K., Zhaparova, S. B., & Alpysbaeva, Z. T. (2023). Dynamics of gas release in highly gassy close-spaced coal seam mining. Gornyi Zhurnal, 2023(3), 60–66. doi:10.17580/gzh.2023.03.09.

[10] Tsai, B. N., & Kolokolov, S. B. (1988). Predicting the Durability of Rocks around Mine Workings. Izvestiya Vuzov (Mining Journal), 41–44.

[11] Chernyak, I. L., & Burchakov, Y. I. (1984). Control of Rock Pressure in Development Workings of Deep Mines. Nedra, Moscow, Russia.

[12] Karetnikov, V. N., Kleymenov, V. B., & Nuzhdikhin, A. G. (1989). Support of main and development mine workings: A handbook. Nedra, Moscow, Russia.

[13] Li, A., Cheng, H., Yue, Z., Rong, C., Wang, P., & Lin, J. (2025). Mechanical performance analysis of fully grouted bolts considering yield and hardening characteristics. International Journal of Rock Mechanics and Mining Sciences, 194, 106197. doi:10.1016/j.ijrmms.2025.106197.

[14] Zadavin, G. D. (2008). Establishing the parameters of bolt (anchor) support for development workings in the mines of the Karaganda basin. Doctoral Dissertation, Karaganda State Technical University, Karaganda, Kazakhstan.

[15] Mustafin, M. G. (1999). Modeling the geomechanical state of rocks surrounding a mine working. St. Petersburg State University of Architecture and Civil Engineering (SPbGASU), St. Petersburg, Russia.

[16] Wang, C., Zheng, X., Xin, W., Wang, J., & Liu, L. (2025). Investigation of Bolt Support Mechanisms and Parameter Optimization for Hard Roof Control in Underground Mining. Processes, 13(1), 94. doi:10.3390/pr13010094.

[17] Demin, V. F., Bakhtybaev, N. B., Demina, T. V., et al. (2012). Prediction of displacements in the near-contour rock mass of mine workings. Mining Information-Analytical Bulletin: Modern Technologies at Mining Enterprises, Special Issue 7, 9–21.

[18] Wang, T., Wang, C., Yang, K., Ren, B., Chi, X., Fu, Q., & Wang, H. (2025). Stability control of roadway surrounding rocks under repeated mining: a case study. Scientific Reports, 15(1), 45187. doi:10.1038/s41598-025-29030-1.

[19] Ren, H., Zhu, Y., Yao, Q., Li, P., & Wei, M. (2025). Study on the mechanism of anchoring parameters of anchor rods in cemented broken surrounding rock. Scientific Reports, 15(1), 28256. doi:10.1038/s41598-025-13442-0.

[20] Dong, J., Ding, W., Qin, Y., & Gao, K. (2025). Safety Status Monitoring of Operational Rock Bolts in Mining Roadways Under Mining-Induced Effects. Sensors, 25(11), 3486. doi:10.3390/s25113486.

[21] Li, Z., Li, J., Shan, R., Liu, J., Tong, X., & Liu, N. (2025). Evolution of surrounding rock distortion energy during closely spaced coal seam mining and innovative coal pillar design method. Scientific Reports, 15(1), 17485. doi:10.1038/s41598-025-02229-y.

[22] Zhang, J., Zhou, X., Liu, X., Fang, L., Guo, X., & Chen, H. (2025). Full process evolution of deformation and seepage coupling in fractured rock under triaxial stress. Scientific Reports, 15(1), 21896. doi:10.1038/s41598-025-04068-3.

[23] Liu, G., Ma, Q., Yang, X., Guo, L., & Li, L. (2025). Consolidation process of uncemented backfill slurry in a mine stope considering hydro-geotechnical properties of rockmass in adjacent stopes. Scientific Reports, 15(1), 24109. doi:10.1038/s41598-025-08369-5.

[24] Kamarov, R. K., & Demin, V. F. (2023). Technology of bolt support for development workings in coal mines: Monograph. Publishing House of Abylkas Saginov Karaganda Technical University, Karaganda, Kazakhstan.

[25] Hower, J. C., & Greb, S. F. (2005). Geologic hazards in coal mining: Prediction and prevention. International Journal of Coal Geology, 64(1), 1-2. doi:10.1016/j.coal.2005.03.001.

[26] Radchenko, S. A., & Matvienko, N. G. (2014). Methods of fast assessment of intensity for methane release from coal and rocks to improve safety. Bezopasnost truda v promyshlennosti (Occupational Safety in Industry), (4), 34–39.

[27] Tang, Z., Yang, S., Zhai, C., & Xu, Q. (2018). Coal pores and fracture development during CBM drainage: Their promoting effects on the propensity for coal and gas outbursts. Journal of Natural Gas Science and Engineering, 51, 9–17. doi:10.1016/j.jngse.2018.01.003.

[28] Cheng, C., Cheng, X., Yu, R., Yue, W., & Liu, C. (2021). The Law of Fracture Evolution of Overlying Strata and Gas Emission in Goaf under the Influence of Mining. Geofluids, 2752582. doi:10.1155/2021/2752582.

[29] Wu, P., Chen, L., Li, M., Wang, L., Wang, X., & Zhang, W. (2021). Surrounding rock stability control technology of roadway in large inclination seam with weak structural plane in roof. Minerals, 11(8), 881. doi:10.3390/min11080881.

[30] Yu, Y., Wang, X., Bai, J., Zhang, L., & Xia, H. (2020). Deformation mechanism and stability control of roadway surrounding rock with compound roof: Research and applications. Energies, 16(3), 50. doi:10.3390/en13061350.